

Comparative Study of External Film Condensation on Inclined Tubes: CFD Analysis vs. SPACE System Code

Taeyeon Min, Jeong Ik Lee *

Department of Nuclear and Quantum Engineering, N7-1 KAIST, 291 Daehak-ro, Yuseong-gu, Daejeon, Korea 34141

*Corresponding author: jeongiklee@kaist.ac.kr

***Keywords** : Small Modular Reactor, Condensation, Pure Steam, Computation Fluid Dynamics, SPACE

1. Introduction

Currently, South Korea's SMR development is in the licensing phase, centered around the innovative Small Modular Reactor (i-SMR), based on the integrated pressurized water reactor (iPWR) design. The key design concept of the iPWR is that the major components of the Nuclear Steam Supply System (NSSS)—including the steam generator (SG), reactor coolant pumps, core, and pressurizer—are contained within the reactor vessel (RV). Notably, the SG features a helical heat exchanger structure designed to enhance heat transfer efficiency and compactness, and the RV is divided into two sections: the outer shell containing the SG and the inner core region. Additionally, unlike conventional large-scale commercial nuclear reactors, a metal containment vessel (CV) is positioned between the containment building and the RV. The i-SMR adopts a dry iPWR design, wherein the CV is maintained under vacuum during normal operation.

A critical feature of the SMR design is its passive safety systems, which enhance the inherent safety of the reactor by relying on fundamental physical phenomena such as gravity, natural convection, and phase change, even in the event of a loss of offsite power or in situations where operator intervention is impossible. The i-SMR's passive safety systems consist of the Passive Emergency Core Cooling System (PECCS), Passive Auxiliary Feedwater System (PAFS), and Passive Containment Cooling System (PCCS) [1]. Evaluating the complex thermal-hydraulic phenomena that arise during the activation of these passive safety systems is crucial for ensuring regulatory approval and operational reliability.

Among the various accident scenarios for the dry iPWR design, an evaluation of the thermal-hydraulic behavior following a rupture of the Modular Makeup & Purification System (MMPS) charging pipe is notably absent [1]. The MMPS is responsible for controlling the purity and volume of the primary coolant. A rupture in the charging pipe, located near the steam generator lower header and penetrating the CV, would cause coolant from the reactor vessel (RV) to leak into the CV. The coolant in the reactor core would then evaporate within the inner section of the RV, rise, and be released into the CV, or descend into the outer section of the RV. The PAFS circulates auxiliary cooling water between the

steam generator heat exchanger tubes and the external cooling tank of the CV, resulting in condensation on the outer surface of the steam generator tubes. Similarly, condensation occurs on the heat exchanger tubes located at the top of the CV in the PCCS. The condensate then descends and recirculates into the reactor core, forming a closed-loop flow path. Figure 1 illustrates this recirculation path for coolant within the CV-RV during an accident scenario.

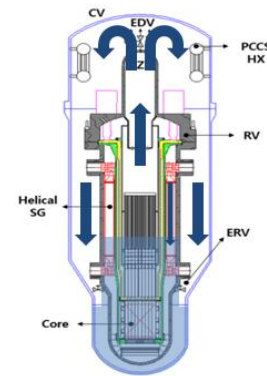


Figure 1. Condensation Scheme at i-SMR in accident

Notably, the condensation of high-pressure pure steam on the outer surface of the steam generator heat exchanger tubes exhibits complex heat transfer characteristics due to the helical structure, but there is a lack of experimental studies or evaluation models simulating these phenomena.

To address this gap, this study develops a framework for analyzing the heat transfer of high-pressure pure steam condensation on the outer surface of the pipe using Computational Fluid Dynamics (CFD). The resulting heat transfer coefficients (HTC) are validated by comparing them with the predictions from the domestic safety analysis code, SPACE, to assess the validity of the model.

2. Methodology

2.1 Preliminary Accident analysis

To define the boundary conditions for the simulations, a preliminary calculation was performed using SPACE v3.3.2 with the i-SMR Basedeck provided by KHNP (2025.09.05). It is noted that since the design of i-SMR

is constantly evolving, the presented simulation results only provide qualitative and approximate results to the actual safety analysis performed for the most up-to-date i-SMR design. The transient simulation was initiated after achieving a steady-state condition. For the critical flow model, the Henry-Fauske/Moody model was selected. Figures 2 and 3 present the calculation results.

In the initial stage of the MMPS charging line break, the rapid decrease of RV pressure and water level triggers a reactor trip signal due to high containment pressure. Subsequently, the SG tubes are exposed to steam resulting from the rupture. Following the activation of the PECCS, the RV and CV pressures rapidly reach equilibrium, after which the pressure continues to decrease due to long-term passive cooling. Ultimately, condensation occurs on the exterior surfaces of the SG tubes. From the system code simulation, the boundary conditions for the CFD simulation are obtained and summarized in Table I, which is representative values after the system reaches pressure equilibrium.

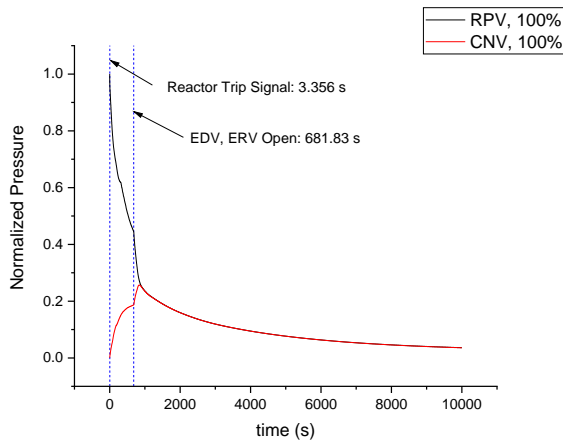


Figure 2. Normalized Pressure

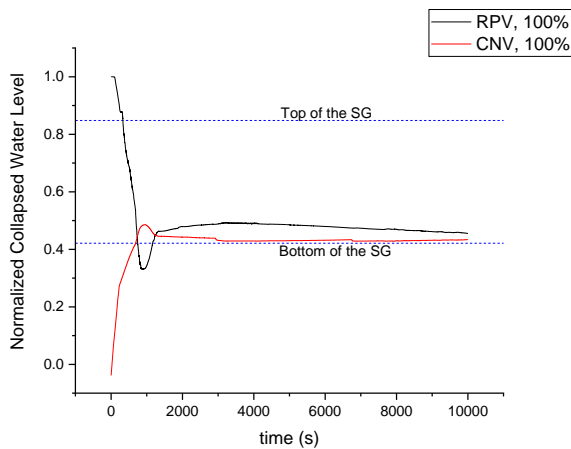


Figure 3. Normalized Water Level

Table I. Boundary condition for CFD simulation

Category	Parameter	Values
General Conditions	Outlet pressure	2.0 MPa
	Inlet velocity	0.1 m/s
	Inlet quality	Saturated steam
	Geometry	$D_o = 15 \text{ mm}, \theta = 20^\circ$
Variable conditions	Wall subcooling (Tube)	Case 1: 3 K
		Case 2: 1 K

2.2 CFD analysis

For simplicity, the computational domain was reduced to a single inclined tube within a rectangular duct. Figure 4 depicts the overall geometry. Saturated steam flows downward, undergoes condensation on the exterior of the pipe located at the center, and subsequently exits the domain. The tube wall was assigned a fixed temperature boundary condition corresponding to the prescribed wall subcooling. The side walls, colored yellow in the figure, were set to symmetry conditions to prevent boundary effects. The front and back walls were assigned no-slip adiabatic boundary condition.

Furthermore, sufficient entrance and exit lengths of 10D and 20D, respectively, were incorporated to ensure fully developed flow and numerical stability. The domain width was carefully optimized to achieve a balance between inlet turbulence resolution and computational efficiency. To establish the initial condition for film condensation, the analytical film thickness for a horizontal tube was determined using the Nusselt equation. Under the specified boundary conditions, the calculated thickness is approximately 0.03 mm.

$$\delta_{F,horizontal} = 1.37 \left[\frac{\mu_l k_l (T_{sat} - T_w)}{g h_{fg} \rho_l (\rho_l - \rho_g)} \right]^{\frac{1}{4}} \quad (1)$$

Figure 5 shows snapshots of the mesh, highlighting refinements near the wall of the tube. To resolve the physics within the liquid film, the mesh was constructed with 10 cells in the radial direction and 240 cells in the azimuthal direction. The total cell count for the domain was approximately 1.29 million.

The CFD simulation was conducted using Ansys Fluent 2025 R1. A Volume of Fluid (VOF) model was selected for the two-phase flow [2]. Moreover, a phase change model and the Continuum Surface Force (CSF) model were adopted to describe behavior of mass and heat transfer of the liquid film [3]. In particular, the phase change model was implemented via the Modified Lee model by Minko et al., in which the relaxation factor is defined based on the energy balance between latent heat and conduction within the liquid film [4][5]. The detailed numerical schemes are summarized in Table II.

Table II. Numerical schemes and model settings for CFD analysis

Category	Discretization and Model	Settings
P-V coupling	Scheme	PISO
Volume Fraction	Scheme	Geo-Reconstruct
	Cutoff value	1e-6
Spatial discretization	Gradient	Least Squares Cell-Based
	Pressure	PRESTO!
	Momentum/Energy	Second Order Upwind
	Turbulent Kinetic Energy	
	Specific Dissipation Rate	
Time discretization	Time Integration	First Order Implicit
	Time Step Size(Δt)	2e-6s
Convergence condition	Residuals	1e-4 for Continuity, 1e-6 for others

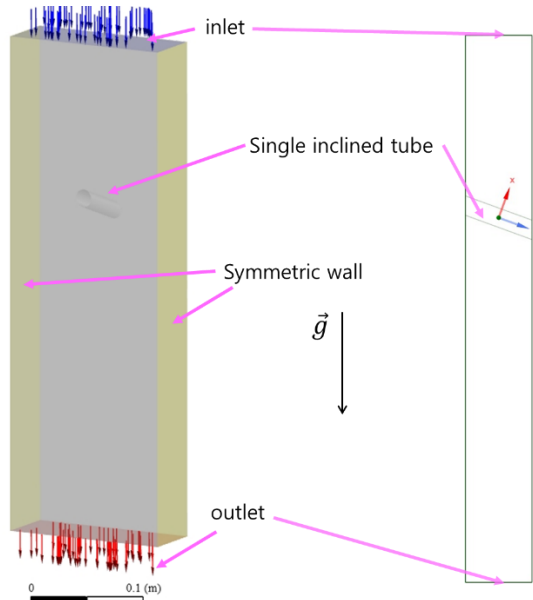


Figure 5. Numerical domain and boundary conditions for a vertical flow duct with a single inclined tube: 3D isometric view(left) 2D side view(right)

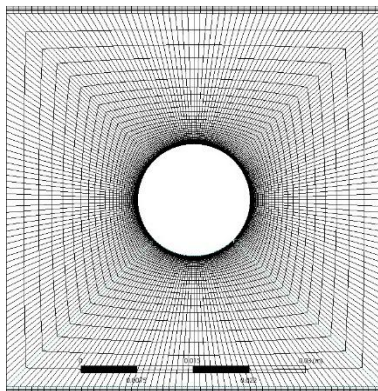


Figure 6. Grid around the condensation tube

2.3 SPACE analysis

For the SPACE analysis, the input was modeled using a computational domain identical to that used in the CFD analysis. Figure 7 illustrates the detailed configuration. Correspondingly, the same boundary conditions were applied to ensure consistency between the two methodologies.

In this nodalization, H310 is defined as the heat structure representing the external surface of the tube where condensation occurs. This component is specifically modeled to facilitate the heat exchange between the steam in the fluid volume and the coolant inside the tube, allowing for the direct comparison of the condensation HTC with the CFD results.

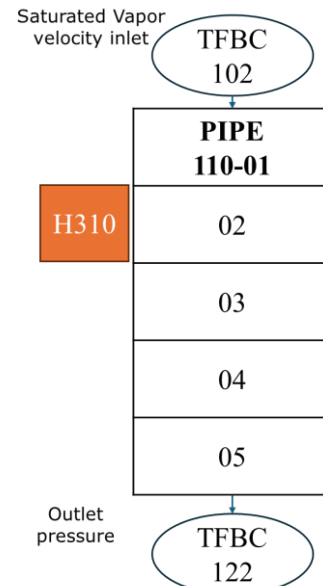


Figure 7. SPACE Modeling configuration

3. Results

The behavior of the liquid film is illustrated in Figure 8. The flow characteristics are distinctively categorized into two regions: the upper film region and the bottom accumulation region. In the upper region, the flow is dominated by gravity-driven circumferential flow. In contrast, the flow in bottom region represents longitudinal flow aligned with the inclination angle. Furthermore, the irregular velocity vectors observed in bottom region indicate the entrainment of liquid film as it accumulates.

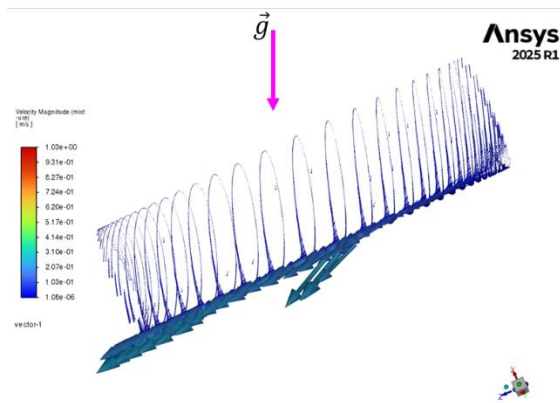


Figure 8. Liquid film velocity vector field ($t=0.4s$)

The CFD analysis results are presented in Figure 9 that for both Case 1 ($\Delta T = 3\text{ K}$) and Case 2 ($\Delta T = 1\text{ K}$), the flow patterns reached a stable steady state within approximately 0.4 seconds following the initial transient period. Similarly, the SPACE code results exhibited rapid convergence, maintaining stable condensation heat transfer behavior (Figure 10). A quantitative comparative analysis between the two computational tools revealed that the SPACE code tends to significantly overestimate the heat transfer performance compared to the CFD results. Specifically, under the $\Delta T = 3\text{ K}$ condition, the condensation HTC derived from the CFD (h_{CFD}) was calculated at $16,500\text{ W/m}^2\text{-K}$, whereas the SPACE code (h_{SPACE}) predicted $33,100\text{ W/m}^2\text{-K}$, which is approximately twice as high. This discrepancy became more pronounced under the $\Delta T = 1\text{ K}$ condition; while the CFD predicted $20,700\text{ W/m}^2\text{-K}$, the SPACE code yielded $54,600\text{ W/m}^2\text{-K}$, a value approximately 2.6 times higher.

Despite these differences in magnitude, both models consistently showed a physical trend where the HTC increases as the wall subcooling decreases, due to the thinning of the liquid film. This consistency supports the fundamental physical validity of both modeling approaches. Consequently, it was confirmed that the existing correlations used in the SPACE system code may over-predict the heat transfer for the complex thermal-hydraulic phenomena associated with high-pressure pure steam and inclined tubes. These findings suggest the necessity of optimizing and improving the precision of the condensation models within the SPACE code through further validation with respect to experimental data. However, the experimental data under these conditions are insufficient and limited.

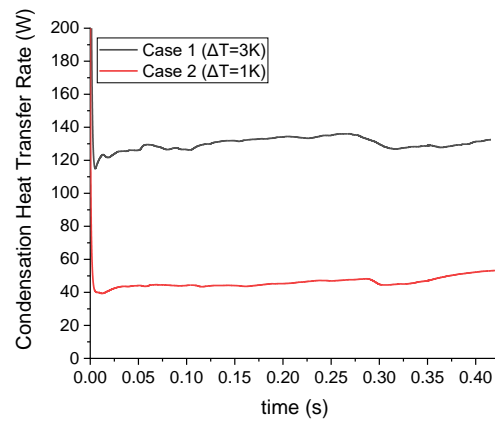


Figure 9. CFD analysis results

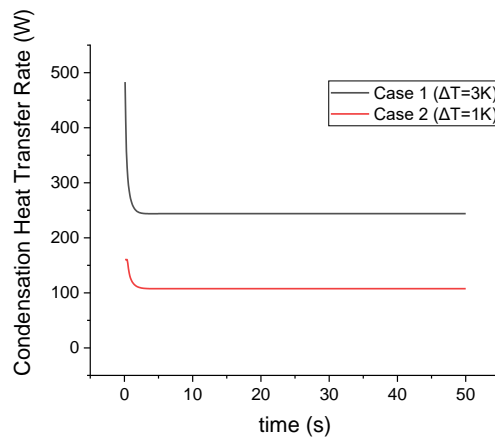


Figure 10. SPACE analysis results

4. Conclusions

The present study established a CFD-based analysis framework to evaluate the condensation heat transfer of high-pressure pure steam on the exterior of an inclined tube, simulating the thermal-hydraulic conditions of an i-SMR accident scenario. The CFD results successfully captured the stable formation of a liquid film and reached a steady state within a short transient period. A comparative analysis with the domestic safety analysis code, SPACE, revealed that while both models consistently predict an increase in the heat transfer coefficient as wall subcooling decreases, the SPACE code significantly overestimates the heat transfer performance by a factor of 2.0 to 2.6. This discrepancy highlights the limitations of existing correlations in system codes when applied to the high-pressure pure steam conditions. The findings of this study provide a critical technical basis for the necessity of optimizing condensation models and suggest that further validation with respect to experimental data is essential to enhance the reliability of SMR safety assessments.

ACKNOWLEDGEMENTS

This work was supported by the Innovative Small Modular Reactor Development Agency grant funded by the Korea Government (MCEE) (No. RS-202400404240).

REFERENCES

- [1] S. G. Lim, H. S. Nam, D. H. Lee, and S. W. Lee, "Design characteristics of nuclear steam supply system and passive safety system for Innovative Small Modular Reactor (i-SMR)," *Nuclear Engineering and Technology*, vol. 57, no. 10, Oct. 2025.
- [2] C. W. Hirt and B. D. Nichols, "Volume of Fluid (VOF) Method for the Dynamics of Free Boundaries," *J Comput Phys*, vol. 39, pp. 201–225, 1981.
- [3] J. U. Brackbill, D. B. Kothe, and C. Zemach, "A Continuum Method for Modeling Surface Tension," 1992.
- [4] W. H. Lee, "A Pressure Iteration Scheme for Two-Phase Flow Modeling," 1979.
- [5] K. B. Minko, V. I. Artemov, and A. A. Klement'ev, "Simulation of Condensation of Stagnant or Moving Saturated Vapor on a Horizontal Tube Using the Volume-of-Fluid (VOF) Method," *Thermal Engineering*, vol. 70, no. 3, pp. 175–193, Mar. 2023.